SHORT NOTE ON THE NOVEMBER 26, 2019, DURRES (ALBANIA) M6.4 EARTHQUAKE: STRONG GROUND MOTION WITH EMPHASIS IN DURRES CITY

by Llambro Duni[1] and Nikos Theodoulidis[2]

(1) Department of Seismology, Institute of Geosciences, Energy, Water and Environment, Politechnic University of Tirana (IGEWE-PUT), Tirana, Albania.

(2) Institute of Engineering Seismology & Earthquake Engineering (ITSAK-EPPO), Thessaloniki, Greece

INTRODUCTION

The November 26, 2019 02:54:12GMT (M6.4) earthquake in Albania, dramatically affected the city of Durres as well as several towns and villages close to the seismogenic zone (epicenter EMSC source: 41.38N, 19.47E, h~10km; epicenter IGEWE source: 41.46N, 19.44E, h~38 km). The earthquake killed 51 people, injured more than 900 and destroyed thousand of buildings in the meizoseismal area.

Apart from Albania, it was felt in Greece, Montenegro, Italy and N. Macedonia. Based on the published fault plane solutions, the earthquake was generated by the activation of a northwest-southeast striking thrust fault. The aftershock sequence until December 26, 2019, included more than 26 earthquakes with magnitude ML≥4.0.

In this preliminary report an attempt is made to understand properties of strong ground motion of the mainshock with emphasis in the city of Durres that paid a large portion of the 'toll' to the total disaster. The first results may show the near future research steps necessary to assure the seismic risk mitigation for the city of Durres and its broader area.

STRONG GROUND MOTION

The earthquake of Nov. 26, was recorded at seven accelerometric stations of the Albanian network, in a range of epicentral distances15km≤R≤130km. In Figure 1 geographic distribution of the stations recorded the earthquake acceleration time histories is shown. In Table 1 information of the recording accelerometric stations as well as recorded peak ground values of peak ground acceleration, velocity and displacement is given.
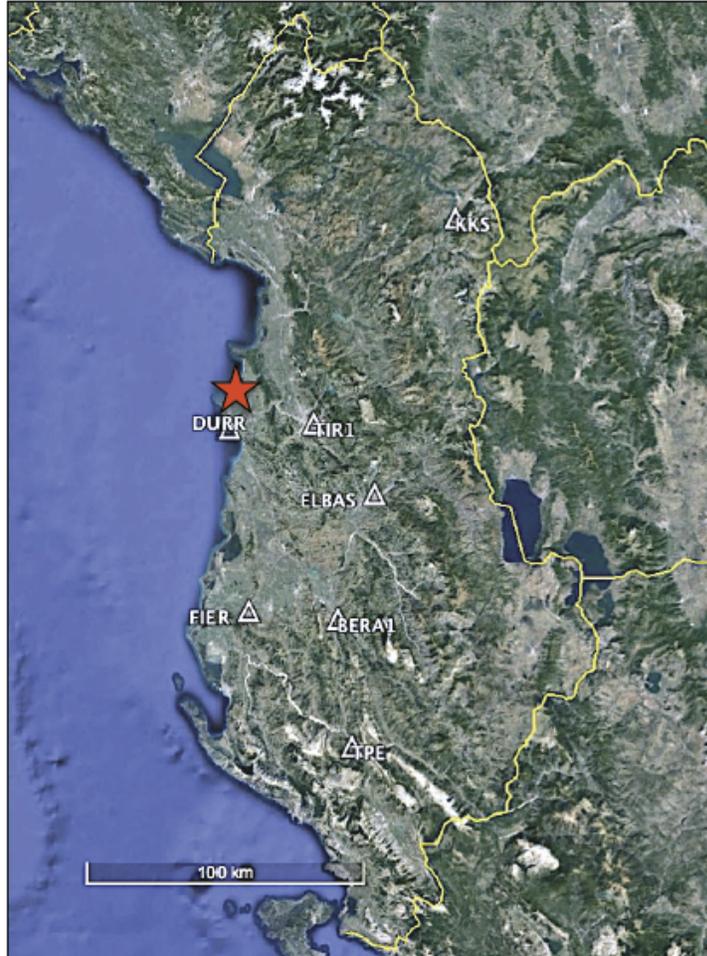
Figure 1. Strong motion stations in Albania recorded the Nov. 26, 2019 earthquake (M6.4), and its epicenter (red star).

In Table 1, epicentral distances are given according to the assessment of hypocenters given by the IGEWE, 41.46N, 19.44E, 38km depth for the November 26, M6.4 event. There are different evaluations given by other agencies, most of which accept focus depth around 20-25 km for the main shock. These differences are thought to be due to the velocity models of the area available at present. In fact, the AlbACa (Albanian Aftershock Campaign) project initiated by GFZ, Potsdam (Schurr at al., 2019) is launched immediately after the November 26 earthquake. In three days, 30 short-period seismometers (20 x 4.5 Hz geophones, 10 x 1 Hz Mark L43D seismometers) were installed in the source region area. Recording is planned for about three months and, among others, we'll have a more detailed velocity model in order to re-locate all the events recorded in this period of time.

In Figure 2, a comparison of recorded PGAs with predicted values based on a regional GMPE (Skarlatoudis et al. 2003) is presented. For the applied GMPE, thrust fault and stiff soil conditions (category C according to NEHRP) are considered. The PGAs of both

horizontal components at the closest to the epicenter DURR station are pointed out for reasons to be explained in the next section.
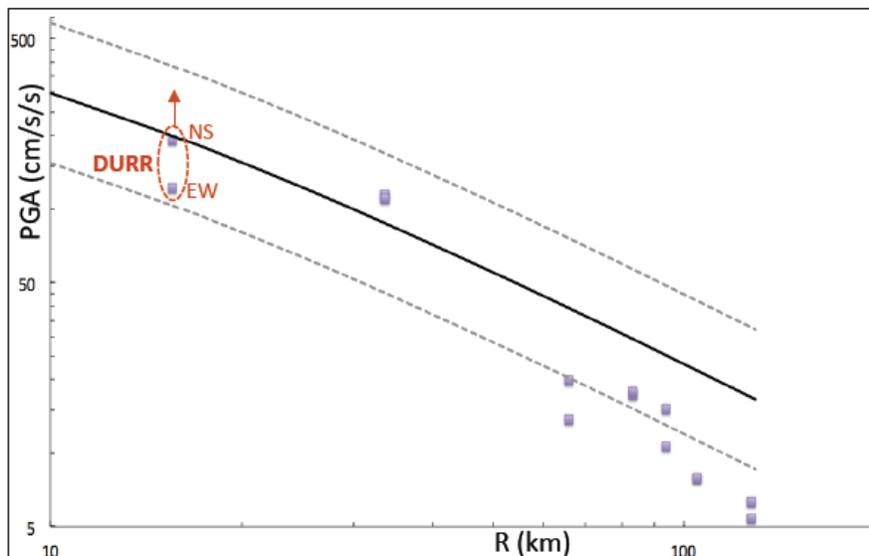

Figure 2. Comparison of recorded PGAs of the Non. 26, 2019 earthquake (M6.4) with a regional GMPE of Skarlatoudis et al. (2003) (solid line:mean, dashed lines:1sd).

Although the number of recorded PGA values are few to lead to conclusion, in general the predictive relation seems to be sufficient for distances shorter than 35km while for distances greater than 65km it systematically overestimates the actual values, remaining close to -1 standard deviation. A possible cause of this trend could be attributed to higher anelastic attenuation of the broader epicentral area compared to the one provided data to define the selected GMPE. Certainly, additional GMPEs must be compared with the recorded values before any solid conclusion is derived.

DURRES ACCELEROMETRIC STATION CHARACTERIZATION AND STRONG GROUND MOTION

The city of Durres is mainly built on recent Holocene marshy deposits, clays, sands, peat with a part of it on Pliocene clays (Figure 3a). The liquefaction potential of the broader residential area was studied by Kociu (2004) and divided in three categories: (1) in areas highly susceptible to liquefaction, (2) areas moderately susceptible to liquefaction and (3) areas with low susceptibility to liquefaction (Figure 3b). In addition, Kociu et al, (1985) produced an equal depth contours map for the city of Durres showed a 3D bedrock morphology implying a 3D basin model (Figure 4).
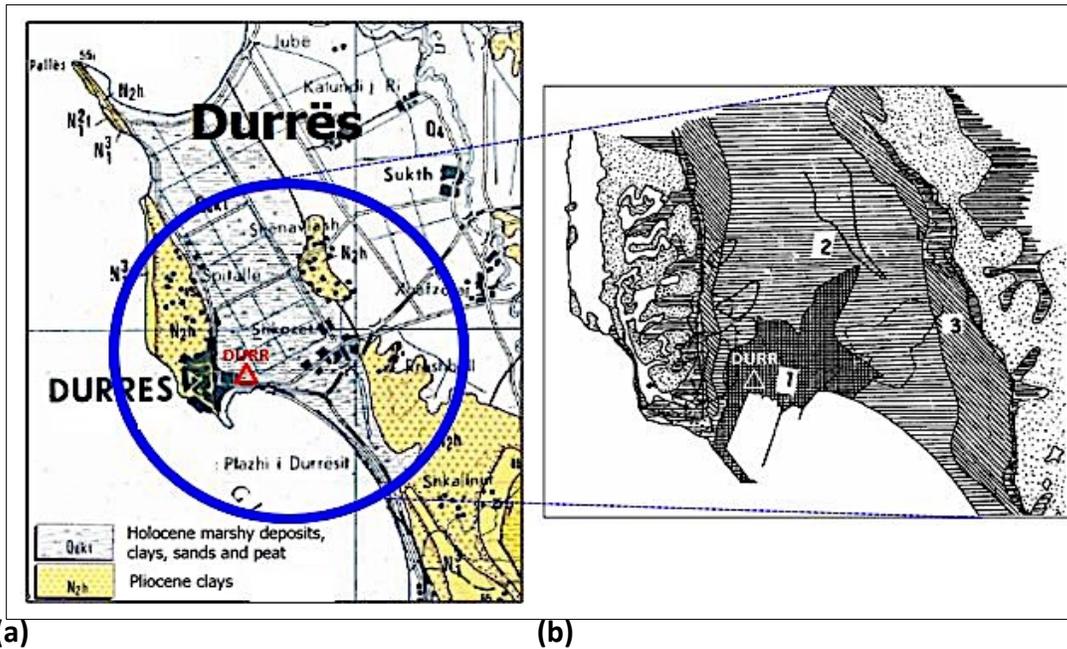
Figure 3. (a) Geological Map of Albania (1983), Scale 1:200.000 (Shehu et al., 1983); **(b)** Liquefaction potential in the Durres city (Kociu, 2004): [1] Areas highly susceptible, [2] Areas moderately susceptible, [3] Areas with low susceptibility.
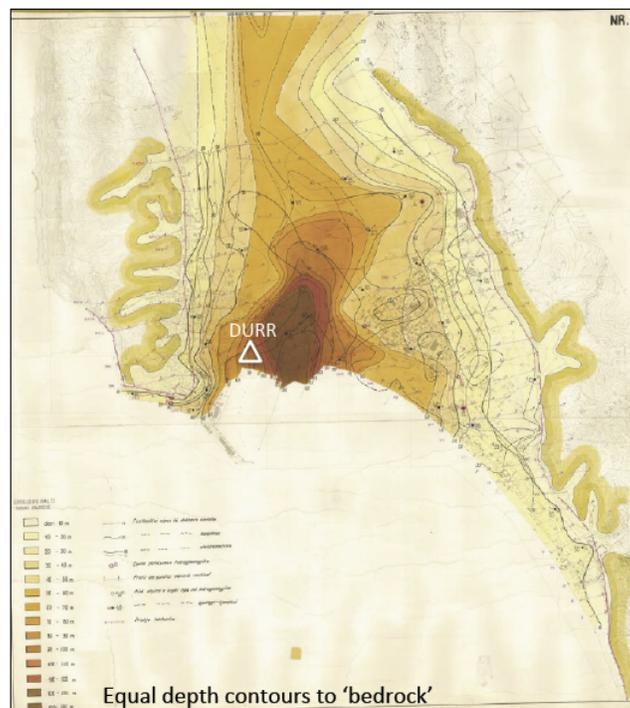

Figure 4. Equal depth to 'bedrock' contours map for the city of Durres according the microzonation project of Durres (Kociu et al., 1985).

The unique accelerometric station DURR, as is shown in Figures 3a, 3b, is installed on soft soil formations (Holocene marshy, clays, sands and peat) in area highly susceptible to liquefaction, in the southwestern part of the basin (Figure 4). In Figure 5 the housing shelter of the DURR station is shown. In Figure 6 an east-west cross section of the basin shows a three-layer structure underlain the station (Koci, 2013). The average shear wave of the uppermost 30m is Vs30≈200m/sec (Duni, 2013), in agreement with the soft surface geologic deposits shown in Figure 3.
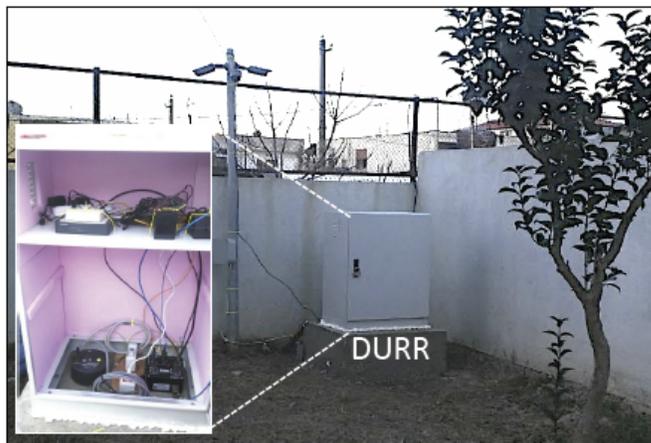

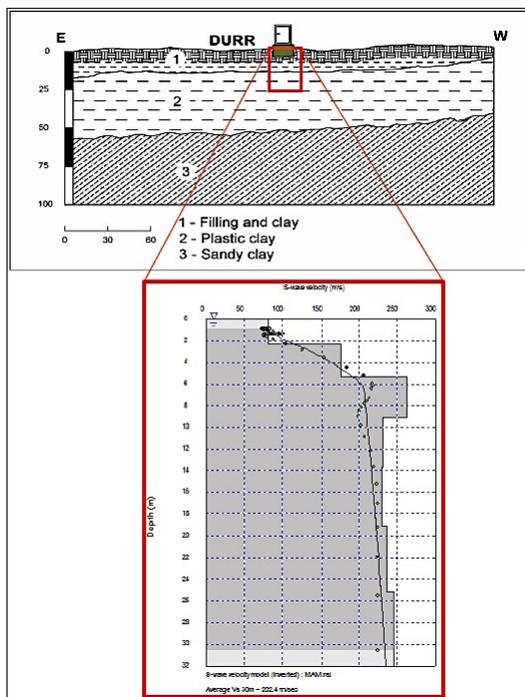**Figure 5.** DURR free-field accelerometric station (CMG-DM24).

Figure 6. East-west cross section and lithology (upper) of the Durres basin (Koci, 2013); Vs profile of the DURR station for the upper 30m (lower) (Duni, 2019).

Due to electricity pause during the mainshock a part of the time history, after the first 15sec, was not recorded at the DURR station, as shown in Figure 7. In the first part of ~15sec, three different types of waves are apparent; the P-waves, the S-waves and another wave arrival of S-waves or/and surface waves. The difference of the latter waves arrival from the initial S-waves is mainly the increase of their amplitude (almost double) and their longer period content.
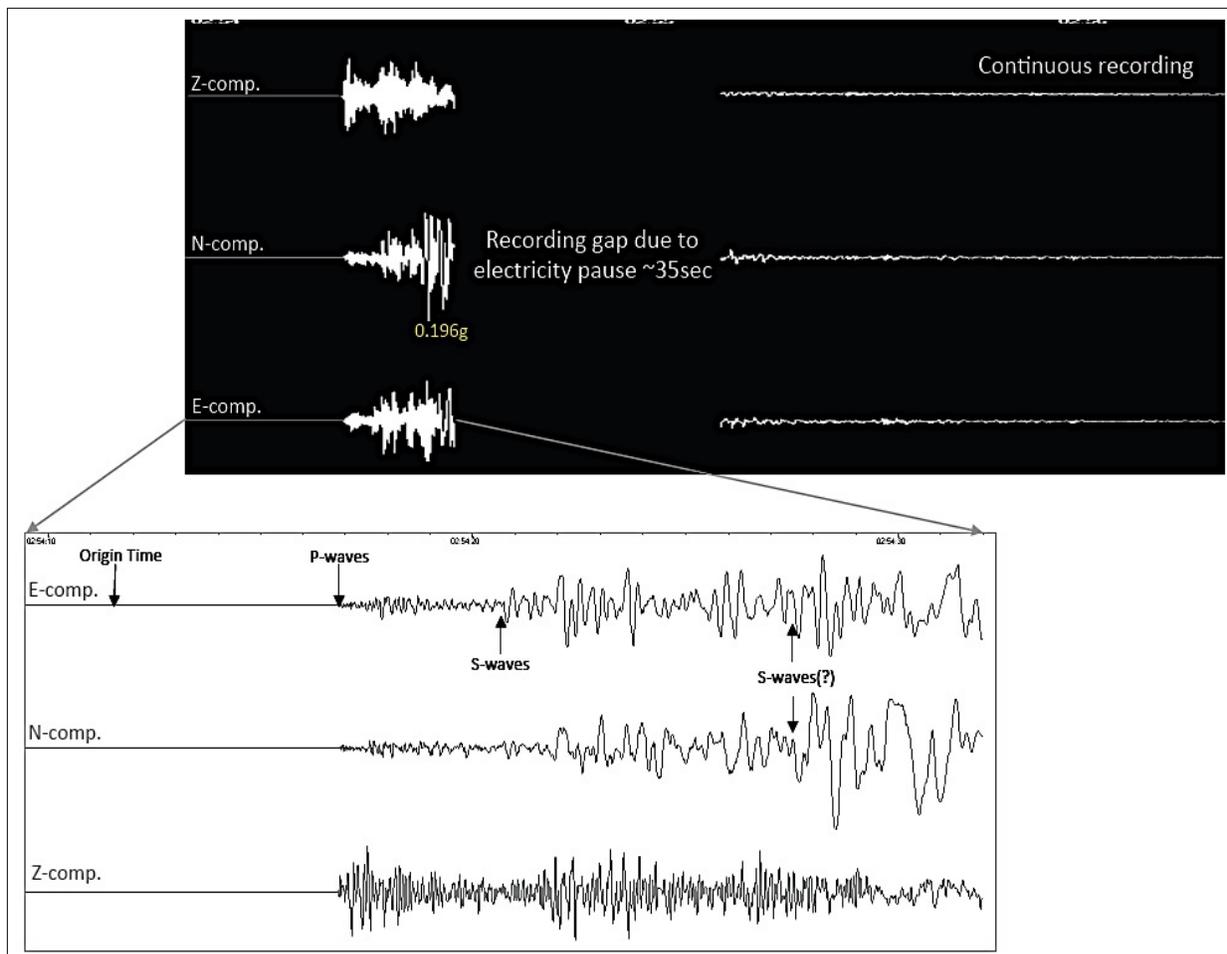

Figure 7. Raw acceleration time history at the DURR station (upper) and a zoom of the first part, ~15sec, of the recording.

In Figure 8 the pseudo-acceleration response spectra, for D=0.02, 0.05, 0.1, 0.2, for the first 15sec of the recording are presented. High acceleration spectral values ≥500 cm/s/s are observed for a wide period range between 0.3sec to 1.0sec. Spectral values remain higher than 300cm/s/s for an even wider period range between 0.2sec to 1.5sec.
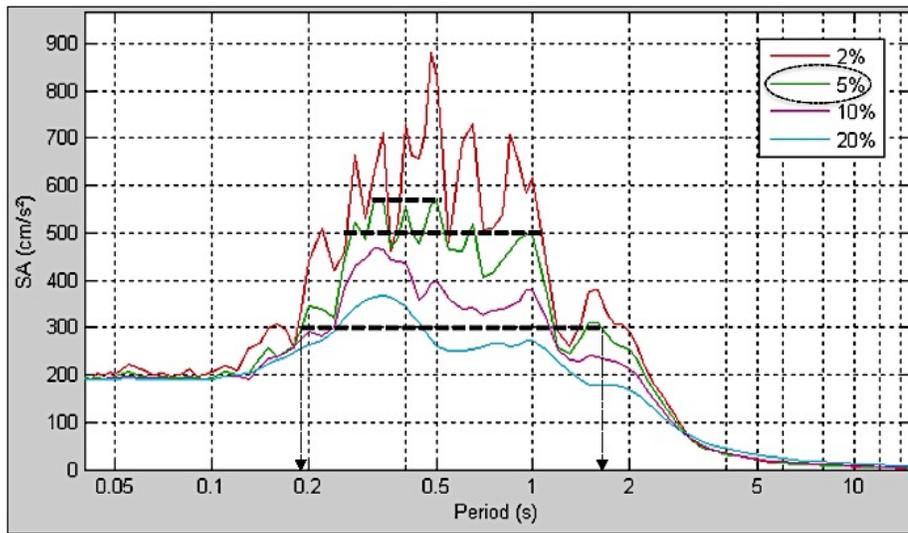
Figure 8. Pseudo-acceleration response spectra (D=0.02, 0.05, 0.1, 0.2) of the first 15sec of the acceleration time history recorded at the DURR station.

This characteristic in combination with the fact that the bracketed duration in horizontal components is at least 11sec with ground acceleration ≥50cm/s/s, could describe the severity of strong ground motion in the Durres city. Provided that the acceleration time history is interrupted about 15sec after its first P-waves arrivals we cannot exclude higher peak ground or/and spectral values within the following 36sec when continuous data recording stopped due to electricity pause. For this reason recorded peak ground values at DURR are highlighted in Table 1 and in Figure 2.

## PERMANENT DISPLACEMENT AND PARTICLE MOTION AT THE DURRES ACCELEROMETRIC STATION

High-resolution digital accelerometers can imprint in the near field permanent displacement due to strong ground motion. The accelerometer of the DURR station was installed at an epicentral distance of ~15km and probably on the hanging wall of the causative fault. However, the latter remains to be proved after relocation of aftershocks and detailed source properties study. For estimation of any possible permanent displacement the first 11sec of the recording, starting from the arrival of P-waves, is used. After baseline correction and double integration of the raw acceleration time histories of all three components, an estimation of average permanent displacement is presented in Figures 9a, 9b and 9c, for the vertical, east-west and north-south components, respectively. For the vertical component it is estimated +1.2cm, in the east-west -1.5cm and in the north-south -5.2cm. Both the vertical and the resultant horizontal permanent displacements are presented on the map of Figure 10. In the same Figure the aftershocks within the first two weeks with M≥2.5 (AUTh, Seismological Station) and the interferogram of the broader seismic fault area according to which the

7
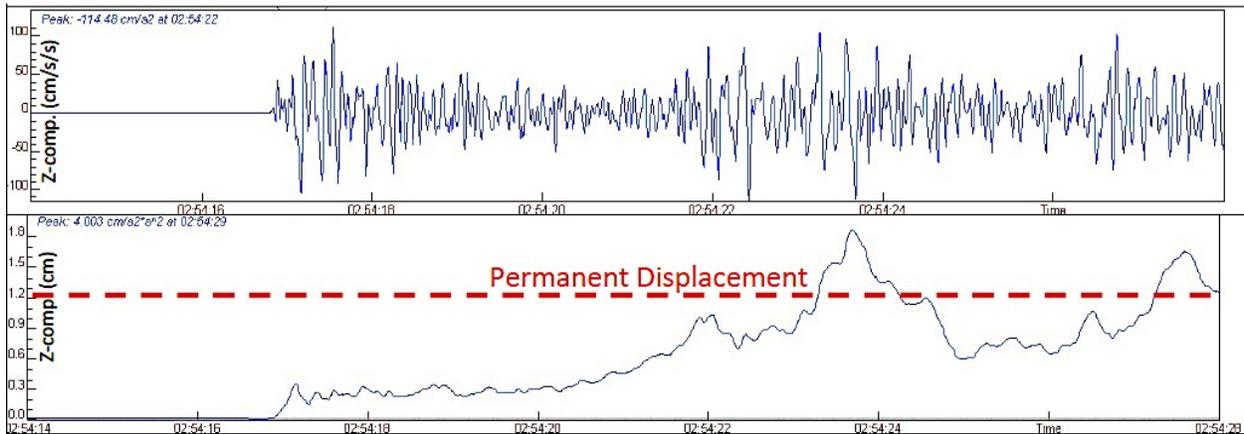
(a)
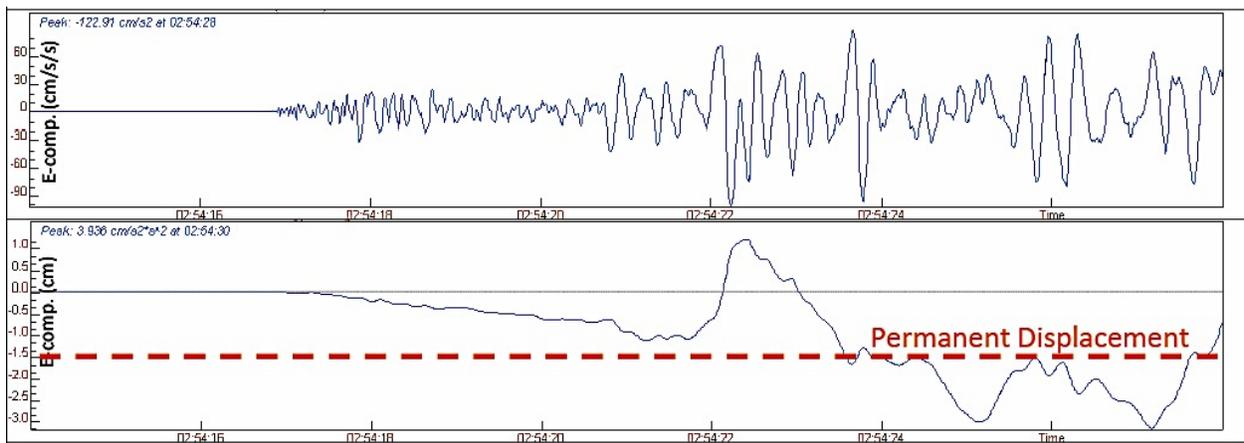
(b)
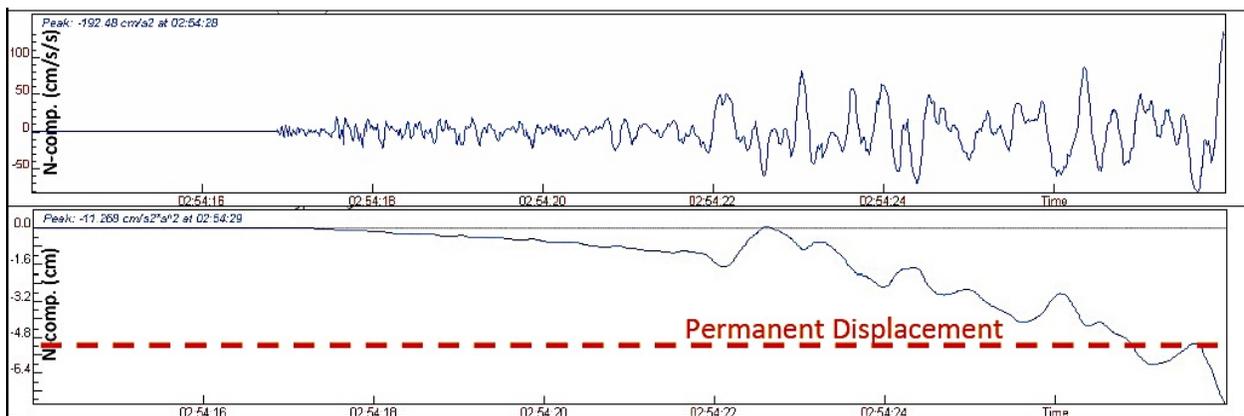
(c)

Figure 9. Acceleration time histories of the first 11sec recorded at the DURR station; (a) vertical, (b) east-west, (c) north-south components and their corresponding average permanent displacements (dashed red line).
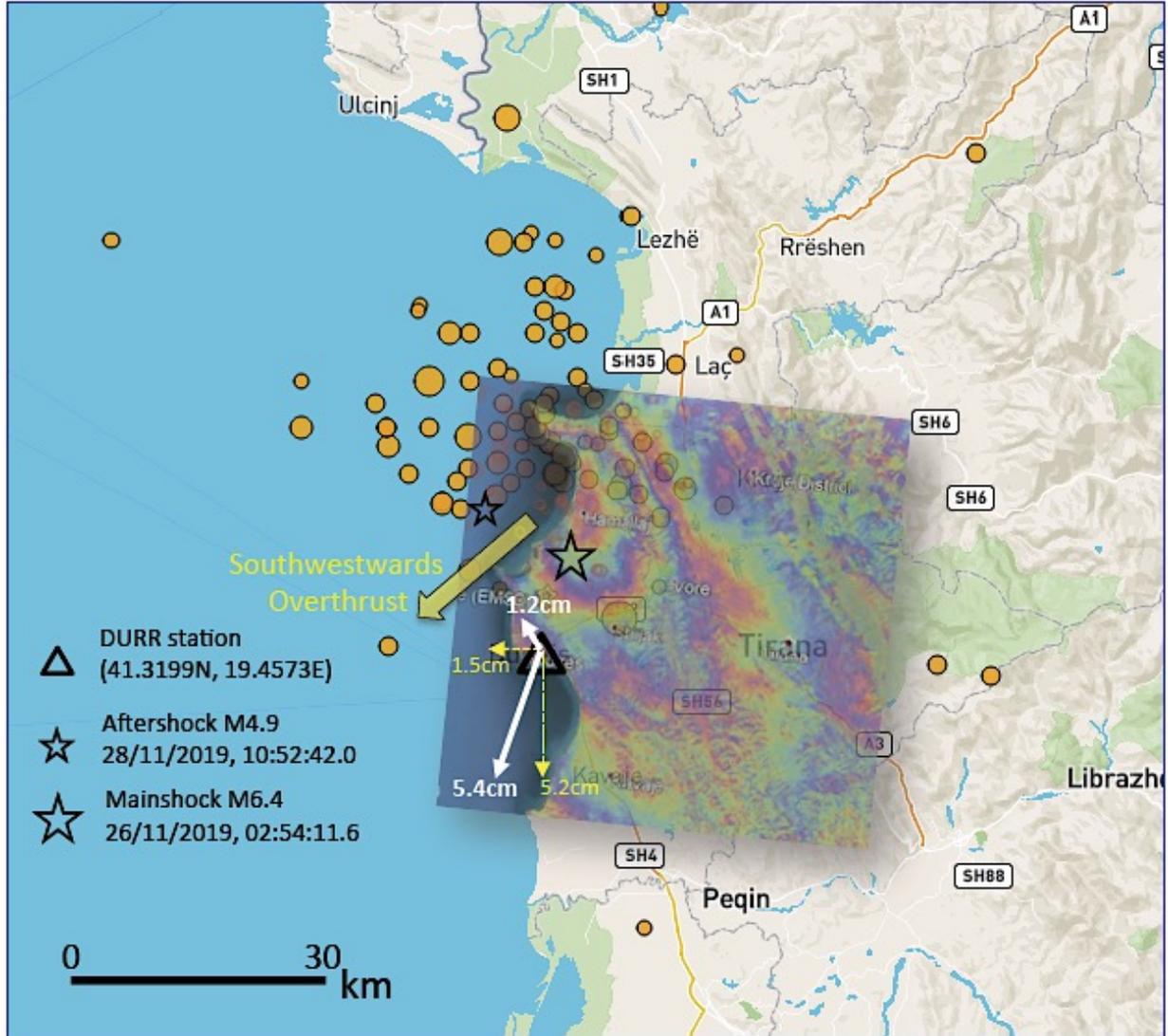
Figure 10. Horizontal and vertical permanent displacements (white arrows) estimated from the acceleration time history of Durres (DURR station); two weeks aftershock activity (AUTh Seismological Station & EMSC); interferogram for the mainshock (Tsironi and Ganas 2019).

vertical uplift close to the epicenter (Hamallaj village) reached a value of 8.4cm (Tsironi and Ganas 2019), are shown. Based on strong ground motion at DURR station the uplift of Durres city is estimated around 1.2cm while the resultant horizontal permanent displacement around 5.4cm towards southwest. Certainly, the aforementioned values must be considered as preliminary and must be compared with any available GPS measurements in the vicinity of Durres.

In Figure 11, the horizontal displacement particle motion separately for both S-wave windows, is calculated. For the first S-wave window a particle displacement of 8cm towards northeast direction (~45°) is clearly observed. However, for the second S-wave window an almost 17cm north-south direction of particle displacement with a simultaneous east-west motion of 8cm is observed. That is, the displacement wave-field is significantly modified moving from one S-wave window to the other.
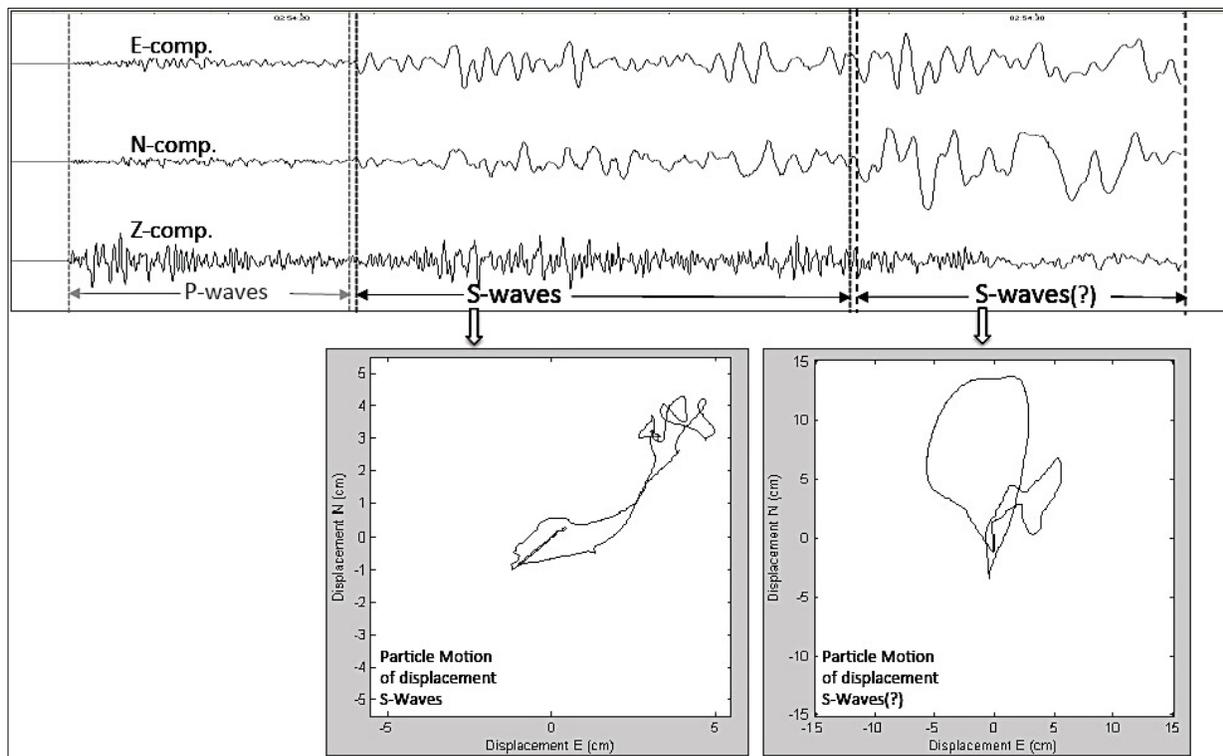

Figure 11. Displacement particle motion at the DURR station estimated for the first S-wave window and the second stronger part of S-wave(?) window of the mainshock.

RECEIVER FUNCTION (HVSR) AT THE DURRES ACCELEROMETRIC STATION

For the city of Durres there was not a reference 'rock' station close by to facilitate estimation of an empirical transfer function and investigate possible soil non-linear phenomena developed during the mainshock strong ground motion. For this reason only the Horizontal-to-Vertical Spectral Ratio (HVSR) method (or Receiver Function) is applicable. To investigate particularities of the dynamic properties of geologic formations beneath the DURR station, the HVSR method applied separately for the first S-wave window and for the stronger part of S-waves (or possibly surface waves) based on the Geopsy software (http://www.geopsy.org).
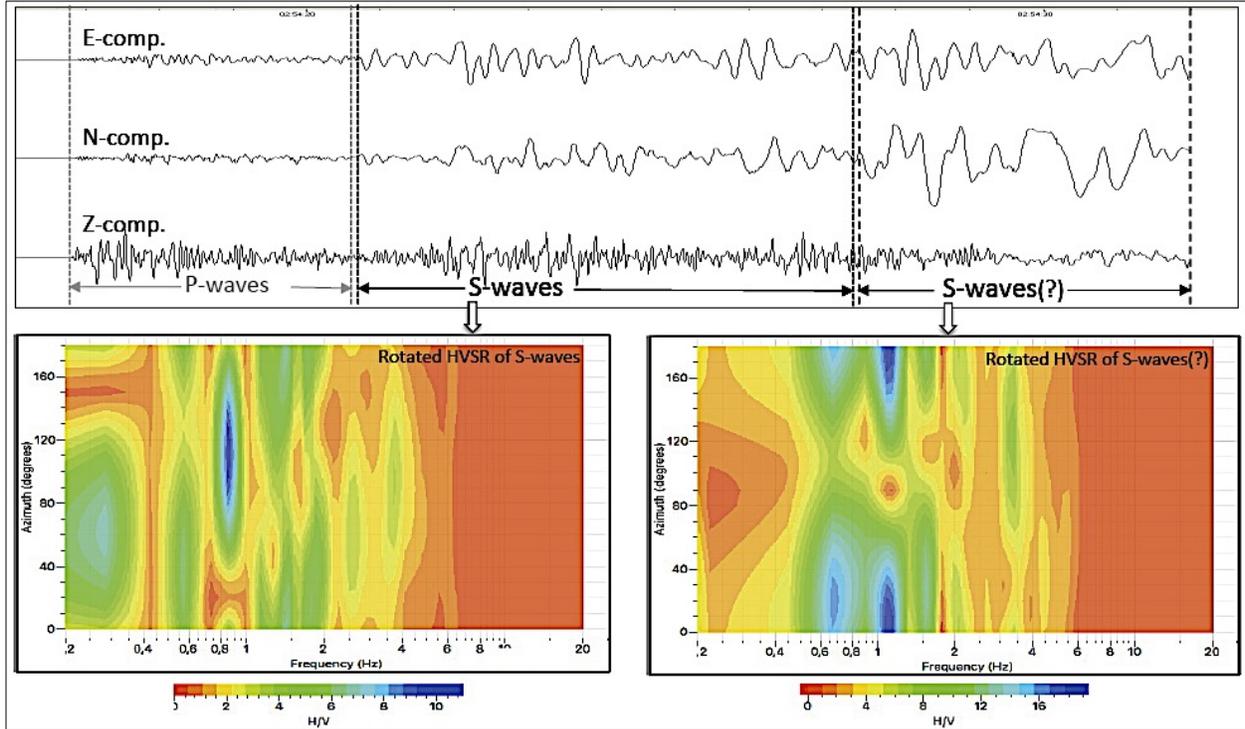
Figure 12. Horizontal-to-Vertical Spectral Ratio (HVSR, Receiver Function) at the DURR station estimated for the first S-wave window and the second stronger part of S-wave(?) window of the mainshock.

For the first S-wave window three HVSR peaks are prevailing at frequency ranges 0.3-0.45Hz, 0.55-0.65Hz, 0.8-1.0Hz and 1.1-1.5Hz with corresponding amplitudes up to 7, 6, 10 and 6, respectively (Figure 12). For the fundamental frequency fo~0.35Hz, its amplitude is preferentially higher in azimuths between 40° to 90°. For the second stronger part of S-wave the fundamental frequency fo~0.35Hz disappears and several HVSR peaks appear at frequency ranges 0.5-0.7Hz, 1.0-1.2Hz and 1.4-1.6Hz with corresponding amplitudes up to 15, 17 and 13, respectively. That is, for the second part of S-waves, in low frequency range (0.5Hz<f<0.7Hz), HVSR amplitudes increases 2 to 3 times compared to the corresponding frequency range of the first S-wave window. It is noteworthy the fact that in the second part of S-waves an additional frequency appears at 1.1Hz with corresponding amplitude up to 17, in azimuths between 0° to 30° and 150° to 180°.

In Figure 13 the HVSR for three time windows of the mainshock is presented; namely, the first S-wave window of 7sec, the second S-wave window of 4.5sec and the entire available record length of 15sec. The striking difference between the HVSR of the first S-wave window and the other two windows is the lack of a frequency peak at 0.3Hz with amplitude 5 that appears in the former. In addition, the amplitudes of the HVSR peaks for the second stronger S-wave window are almost double compared to the ones of the

first S-wave window. However, using the entire available record length, 15sec, the clear HVSR peaks reduce to three; at 0.65Hz, 1.4Hz and 3.5Hz with corresponding amplitudes 12, 10 and 3, respectively.
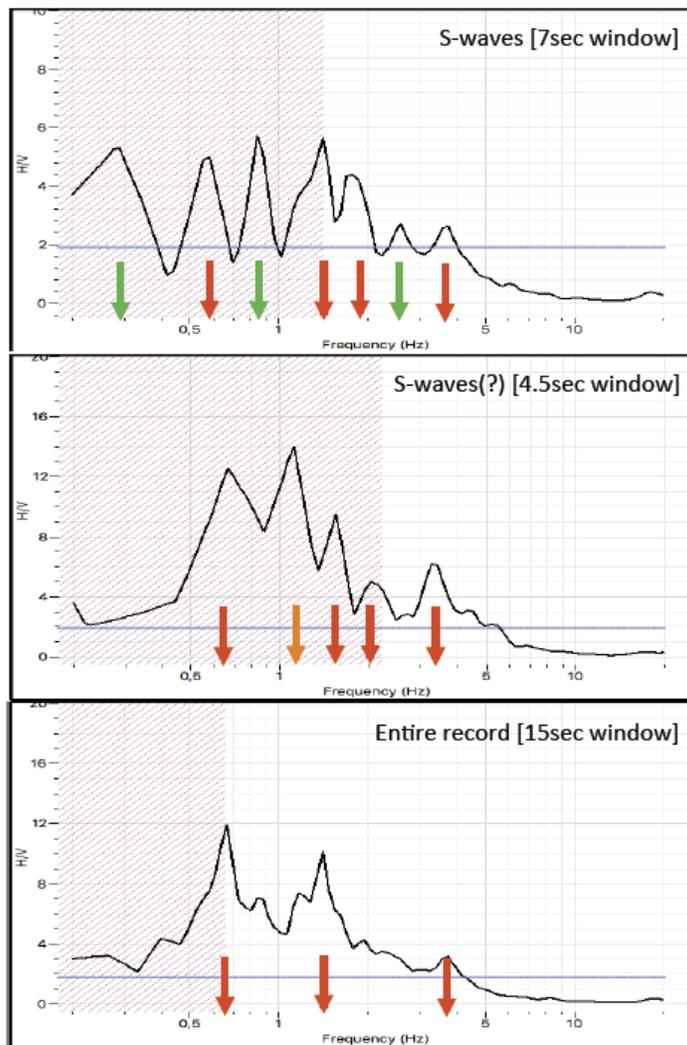

Figure 13. Horizontal-to-Vertical Spectral Ratio (HVSR, Receiver Function) at the DURR station estimated for the first S-wave window(upper), the second S-wave(?) window (middle) and the entire record length of the mainshock (down).

In order to examine the HVSR at DURR station based on low amplitude ground motion, an aftershock recording with PGA equals 72cm/s/s in E-comp., 45cm/s/s in N-comp. and 17cm/s/s in Z-comp. was selected (earthquake of 28/11/2019 10:52:42GMT, 41.47N, 19.35E, M4.9, see Fig. 10). For the HVSR analyses S-wave window of 20sec and surface & coda wave window of 60sec, were selected (Figurer 14). For both windows two prominent peaks appear at 0.3-0.35Hz and 0.5-0.6Hz with amplitudes ~30% reduced in the case of surface & coda waves window.
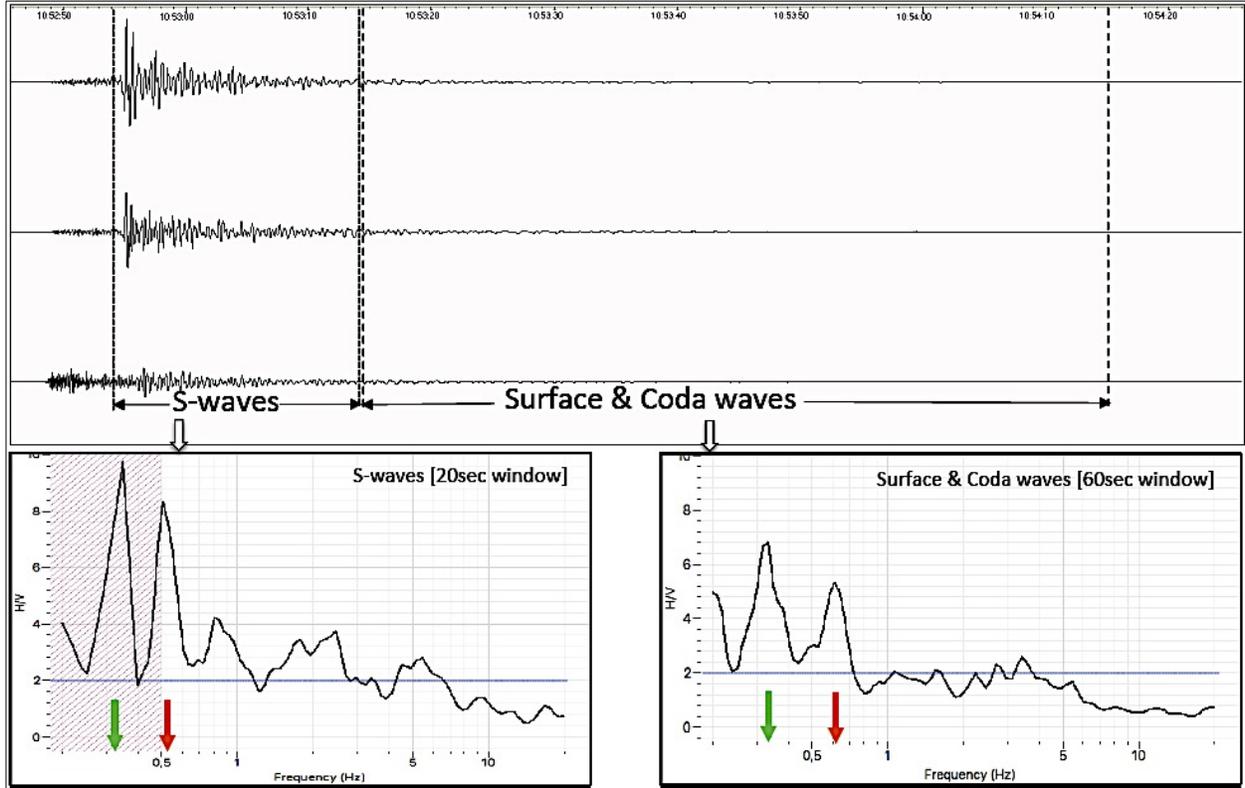
Figure 14. Horizontal-to-Vertical Spectral Ratio (HVSR, Receiver Function) at the DURR station estimated for the S-wave window and the surface & coda waves window of the aftershock of 28/11/2019, 10:52:44 (M4.6).

These two peaks are also apparent in the case of the first S-wave window of the mainshok (Figure 13) while the second peak at 0.5-0.6Hz is apparent in all three windows of the mainshock. For the case of S-waves window of the aftershock, another three HVSR peaks appear at 0.8-0.9Hz, 1.5-2.5Hz and 4.5-5.5Hz with relatively low amplitudes 3 to 4.

DISCUSSION

In this short note, strong ground motion due to November 26, 2019 M6.4 earthquake in Durres (Albania) is presented. Emphasis on the Durres station (DURR) recording and its site characterization metadata are presented.

The acceleration time history, although is lacking a part of S & surface waves, can be proved significant for many reasons:

- The horizontal PGA 192cm/s/s, in good agreement with the average predicted value by a regional GMPE.
- The spectral acceleration was high, at least 500cm/s/s, for a wide range of periods between 0.3sec and 1.0sec, possibly with decisive impact on a wide range of buildings.

- Its initial 15sec showed that the DURR station shifted southwestwards at least 5.4cm and uplifted 1.2cm.
- The resulting displacement particle motion indicated during the first S-waves window of 7sec, a ~45° north-east motion of 8cm, while for the following 4.5sec the particle motion became almost north-south direction of 17cm.
- The HVSR (receiver function) analyses showed several peaks with high amplitudes (5 to 15) for both the mainshock and an aftershock recordings. From these analyses it seems that non-linear soil behavior was not apparent in the DURR station. Certainly, such a conclusion is very preliminary and needs further investigation.

Taking into account the preliminary results of this short note, the following steps forward could be proposed:

- The properties of 3D basin underlain the city of Durres must be investigated either in situ or in laboratory test. As a first step ambient noise measurements could be carried out in the city and its extension.
- After the source model and slip distribution are defined, strong ground motion simulation can be attempted. The mainshock record at DURR station could be one control point of the simulation results. In addition, future earthquake scenarios from other seismic sources would significantly contribute to seismic design of building and critical infrastructures in the city of Durres and its suburb.
- Among others, all aforementioned efforts would in turn mitigate seismic risk for the city of Durres and increase its resilience against future earthquake disaster.

REFERENCES

Duni Ll. (2013). MASW measurements for the characterization of the Albanian Seismological Network stations. Internal report, IGEWE, Tirane, Albania

Koci R. (2013). Geological characterization of the Albanian Seismological Network stations. Internal report, IGEWE, Tirane, Albania

Koçiu S, Sulstarova E, Aliaj Sh, Duni Ll, Peçi V, Konomi N, Dakoli H, Fuga I, Goga K, Zeqo A, Kapllani L, Kozmaj S, Lika M. (1985). Seismic microzonation of Durresi town, internal report, (in Albanian), IGEWE, Tirane, Albania.

Kociu S. (2004). Induced Seismic Impacts Observed in Coastal Area of Albania: Case Studies, Proceedings of Fifth Int. Conf. on case histories in Geotech. Eng., New York, NY, April 13-17, 2004

Schurr B., Duni Ll., Dushi E., Rohnacher A., Gjuzi O., Kosari E. (2019). Albania Aftershock Campaign (AlbACa), project of GFZ Potsdam and IGEWE Tirane.

Shehu R., Shallo M., Kodra A., Vranaj A., Gjata K., Gjata Th., Melo V., Yzeiri D., Bakiaj H., Xhomo A., Aliaj Sh., Pirdeni A., Pashko P. (1983). Geological Map of Albania in scale 1:200.000, "Hamit Shijaku" Publishing-House, Tirane.

Skarlatoudis A., Papazachos C., Margaris B., Theodoulidis N., Papaioannou Ch., Kalogeras I., Scordilis E. and Karakostas V. (2003). Empirical peak ground motion predictive relations for shallow earthquakes in Greece, Bull. Seism. Seism. Am., 93, 6, 2591-26

Tsironi V. and Ganas Ath. (2019). Wrapped Interferogram of the 26/11/2019 M6.4 Earthquake, Albania-Adriatic Sea, Institute of Geodynamis, Athes, Greece.

Table 1. Information of the accelerometric stations recorded the event of Nov. 26, and corresponding peak ground values

Recording Station				November 26, 2019 Event (M6.4)									
				Epic. Dist.	E-W Component			N-S Component			Z Component		
Code	Site	Instrument	Vs30 m/s	(km)	Pga cm/s2	Pgv cm/s	Pgd cm	Pga cm/s2	Pgv cm/s	Pgd cm	Pga cm/s2	Pgv cm/s	Pgd cm
BERA1	Free field	Guralp: CMG-DM24	1010	93.7	15.10	0.92	0.29	10.65	0.68	0.16	7.91	0.53	0.13
DURR	Free field	Guralp: CMG-DM24	200	**15.6**	**122.3**	**14.4**	**4.52**	**192.0**	**38.55**	**14.0**	**114.5**	**7.18**	**4.39**
ELBAS	2 story building (with a pillar)	Guralp: CMG-DM24	405	65.8	13.69	0.87	0.22	19.75	1.70	0.44	11.88	0.96	0.23
FIER	2 stories building (without pillar)	Guralp: CMG-DM24	375	83.2	17.39	1.50	0.59	17.83	1.20	0.57	8.80	0.74	0.35
KKS	Small 1 story build (with a pillar)	Guralp: CMG-DM24	750	105	7.87	0.95	0.51	7.87	0.79	0.40	-	-	-
TIR1	Free field	Guralp: CMG-DM24	310	33.7	113.9	7.57	1.80	110.0	6.65	1.77	43.49	2.16	0.73
TPE	2 stories building (with pillar)	Guralp: CMG-DM24	690	128.2	5.36	0.72	0.26	6.28	0.79	0.22	3.88	0.37	0.11